Preprints of the 21st IFAC World Congress (Virtual)
Berlin, Germany, July 12-17, 2020

Effect of Direct Slicing on Precision Additive Manufacturing

Hossein Gohari* Ahmad Barari*
Hossam Kishawy* Marcos S.G. Tsuzuki**

** Faculty of Engineering and Applied Science, University of Ontario Institute of Technology (UOIT), Oshawa, Ontario, Canada (e-mails: hossein.goharibahabadi@uoit.ca, ahmad.barari@uoit.ca, hossam.kishawy@uoit.ca)*
*** Escola Politécnica da Universidade de São Paulo, São Paulo, Brazil (e-mail: mtsuzuki@usp.br)*

Abstract: An intelligent process planning for additive manufacturing (AM) is proposed in a paper presented at IFAC-IMS 2019[1]. An important aspect of the intelligent process planning is to directly slice CAD models to generate paths for AM machines. In this paper an experimental approach is carried out to investigate the improvements in the results of fabrication using direct slicing approach. In the proposed process, a CAD model is directly sliced and layer contours are extracted from the ideal surface. The curvature based parametrization using a multi-step method is implemented for finding the position of layers. The dimensional errors are investigated first by comparing the errors generated during the tessellation process with the ideal surfaces. Then the results of printing using paths generated from STL files and the ideal surface defined in an IGES file are compared. The results show considerable improvements in surface continuity and dimensional accuracy of the parts fabricated form the direct slicing approach.

Keywords: NURBS Surface, additive manufacturing, adaptive slicing, cusp volume, geometric complexity, volumetric deviations, direct slicing,

1. INTRODUCTION

Additive manufacturing (AM) is the most promising manufacturing method to produce highly customized and complex parts which are the trend in new industrial designs. Based on the current status of AM methods, these methods are being used for applications such as proof of concepts, spare part production, moulding patterns for precision metal casting. In a common practice, an AM process starts with defining a computer-aided design (CAD) model in digital environment. The model can be defined based on the results of scanning data from an actual object or can be defined based on design specifications. Different methods are developed for surfaces constructions in digital environment. Boundary representation (B.rep) is one of the common approach for surface representation in which a surface is defined based on a collection of primitive or freeform sub-surfaces such as triangles or parametric surfaces.

The most common approach to define a surface in digital environment is to use triangles for construction of model surfaces. The format defined for this type of representation is called stereo-lithography file (STL file). The problem with this type of surface representation is the approximation process in defining the ideal model surfaces by the triangles which causes the chordal errors. This problem is more substantial when the geometric complexity of the ideal model increases. The number of triangles that are needed for defining a complex geometry is exponentially increases by reducing the chordal error for the process of tessellation. Adaptive approaches for generating STL file are developed to reduce the chordal errors (Angelo & Stefano, 2010; "Enhanced stl," 2006; Lalehpour & Barari, 2017; Umaras & Tsuzuki, 2017). The other approach is to use curved triangles and freefrom patches for the process of tessellation (Hiller & Lipson, 2009; Paul, Design, & 2015, n.d.).

The computation time of the slicing procedure is highly dependent on the number of triangles. To minimize the computation time for a specific number of triangles, Minetto et al. (Minetto, Volpato, Stolfi, Gregori, & da Silva, 2017) developed an algorithm in which the triangles are sorted and filtered for each layer.

To eliminate the chordal errors generated in the tessellation process, direct approaches to find the sections of the ideal model are developed. These methods are based on two main approaches which are 1) subdivision based algorithms 2) tracing based algorithms. In the subdivision based algorithms, part sections are extracted by comparing and subdividing the ideal surface with slicing planes (Starly, Lau, Sun, Lau, & Bradbury, 2005). The process of finding the section points in the tracing approach is based on a starting point and a tangent vector defined on the slicing plane. Next points are calculated based on small steps determined based on the location and the specific tangent vector at the previous points (Barnhill & Kersey, 1990; Farouki, Tsai, & Yuan, 1999; Feng, Fu, Lin, Shang, & Li, 2018). The main drawback of using subdivision based algorithm is the computation time to extract the sub-surfaces representing the intersections. To increase the speed on subdivision based algorithm, a method is presented that intelligently subdivides the unimportant part of a surface before starting of the subdivision based algorithm (Hossein Gohari, Barari, & Kishawy, 2018). The numerical stability of the subdivision based algorithms is more than the tracing based algorithm specifically at the surface boundaries.

[1] The paper is available at : https://doi.org/10.1016/j.ifacol.2019.10.067

Next step in an AM process is to calculate the layer thickness based on the complexity of the parts. Currently, the common approach is to find the layer thicknesses uniformly along the z axis of the part. As reported in (Hayasi, Asiabanpour, Hayasi, & Asiabanpour, 2013; Tyberg & Bøhn, 1998), the main drawback of the implementation of adaptive slicing is the determination of process parameters for the curing and sintering the material at different heights. However, implementation of an adaptive approach for the process of layer thickness determination considerably increase the efficiency of the process in terms of building time and accuracy. In addition, using adaptive slicing provides the possibility of using maximum layer thicknesses which improves the homogeneity of the final part.

The part boundaries in an AM process are approximated using some steps along z axis. An algorithm is required to evaluate the length of these steps. First, a criteria is needed to determine the amount of the deviations between the ideal CAD model and the resulting process planned model. Different criterion are introduced to estimate the final part deviations such as cusp height (Dolenc & Mäkelä, 1994), cusp volume (Kumar & Choudhury, 2005) and surface roughness measures (Pandey, Reddy, & Dhande, 2003). Because of the sophistications to calculate the cusp volume in 3 dimensional (3D) space, 2D approaches (cusp height and surface roughness criterion such as Ra) are used to determine the deviations. To determine the surface roughness more accurately, Lalehpour and Barari (Lalehpour & Barari, 2018) presented an algorithm to accurately find the centreline of the deviations for estimation of Ra value. The accuracy of the 2D criterion considerably reduces when complex geometries need evaluation in 3D space. Another approach is simplify the 3D geometry based projections on different planes such as top or side views (Hayasi et al., 2013). The simulation of the deviations also is needed for surface topography and roughness evaluation in 3D space for the inspection process of final parts (Barari, Kishawy, Kaji, & Elbestawi, 2017; Jamiolahmadi & Barari, 2014).

The other approach to determine the layer thicknesses is to use the analytical data extracted from the ideal surface such as instant slope and curvature. To find the layer heights based on the analytical information, multi-step methods are used for the parametrization of ideal surfaces (H Gohari, Barari, & Kishawy, 2016). In addition to deviations, cost and time also can be considered as the criteria for the process of slicing for optimizing layer thicknesses globaly (Sikder, Barari, & Kishawy, 2015a, 2015b).

This paper seeks to implement the direct slicing part of the intelligent process planning for AM processes presented in (Hossein Gohari, Barari, Kishawy, & Tsuzuki, 2019). An optimized aerofoil is constructed for the case studies. Based on the available information for the sections of the aerofoil, NURBS curves are fitted to the reference points. A NURBS surface is defined based on the constructed sections. To compare the results of fabrication using continuous surface and tessellated surfaces, three STL file with different chordal errors are extracted for the continuous model. The results of printing of each STL file are compared with the result of fabrication using the direct slicing approach.

2. PART GEOMETRY DEFINITION

To investigate the effect of direct slicing on accuracy of the final part a case study is designed. Using NURBS interpolation a surface is fitted to the sections reported in ("EP1259711B1 - Aerofoil for an axial flow turbomachine - Google Patents," n.d.). The sections are constructed using NURBS interpolation with the uniform parametrization of the reference points. Two intermediate sections of the aerofoil are interpolated using linear NURBS interpolation of the other three sections to make the shape smoother. The two section are extracted based NURBS surface interpolation of the original three sections.

To generate the curve form the presented data, first the corresponding parameters for reference points should be determined. Chord length method is used to select the parameters for the reference points as shown in Equation (1).

$$u_i = \frac{\sum_{j=1}^{j=i} |Q_{j+1} - Q_j|}{\sum_{j=1}^{j=n-1} |Q_{j+1} - Q_j|} \quad (1)$$

Where Q_j are the coordinates of the reference points and n is the number of reference points. After the determination of the parameters for the reference points, the corresponding values of basis function need to be determined. To define the basis function, a knot vector should be defined based on the degree of and the number of control point of the desired NURBS curve. To define the NURBS curves for the sections, 25 control points are determined for the process of interpolation. The degree of the curve is considered as p=2. Thus, the knot vector will have 28 knots based on the relation that exist between the number of knots and the number of control points and the degree of the NURBS curve.

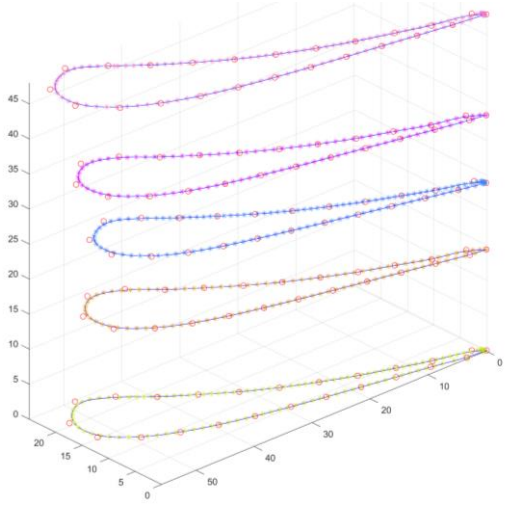

Fig. 1. Aerofoil sections based on data presented in ("EP1259711B1 - Aerofoil for an axial flow turbomachine - Google Patents," n.d.)

The control points of the fitting NURBS curve can be determined using the defined parameters and basic functions based on the following equation (Lain, 2010):

$$[P] = [[N]^T[N]]^{-1}[N]^T[D] \quad (2)$$

Where $[N]$ is the matrix of the determined basis functions for each parameters and $[D]$ is the matrix of the reference points coordinates. Fig. 1 shows the results of NURBS interpolation for the section reference points. The continuity of the defined NURBS curves at each knot position is equal to C^1 which considerably more smooth that the sharp deviation which happens at C^0 continuities. The C^1 continuity means that any defined tangent vector at each point has the same direction and magnitude while in C^0 the value and direction is different. Fig.2 represents the results of NURBS surface fitting for the determined curves. The continuous surface is extracted by storing it at the initial graphics exchange specification (IGES) file. The continuous model then is tessellated using triangles with three different chordal errors (chordal Tol. =0.05 mm, chordal Tol. =0.1 mm and chordal Tol. =0.2 mm). Then using a surface fitting algorithm, deviations of the tessellated surfaces are compared with the ideal surface.

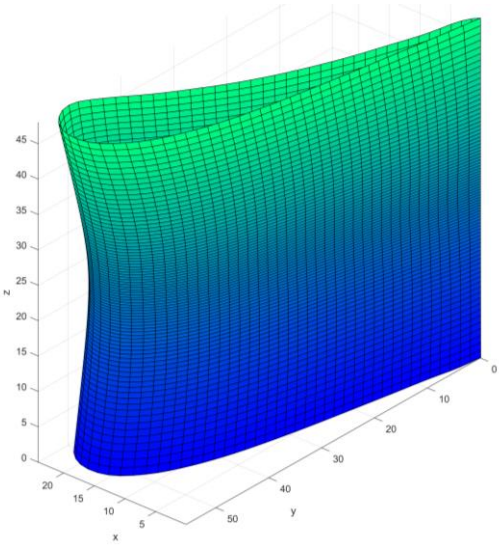

Fig. 2. Aerofoil reconstructed based on the section data presented in ("EP1259711B1 - Aerofoil for an axial flow turbomachine - Google Patents," n.d.)

The edge points of the triangles are directly extracted for the ideal surface therefore they do not have any deviations. To complete the procedure first the triangles are subdivided to find the intermediate points inside the triangles. Table 1. Shows the results of the deviations in tessellation with different chordal errors. In the next step, these models are sliced and printed to evaluate the accuracy of the parts using the determined tessellation parameters. The fused filament fabrication (FFF) method was used to fabricate the samples with Polylactic acid (PLA) material. The Prusa MK3S ("Original Prusa i3 MK3S - Prusa3D - 3D Printers from Josef Prusa," n.d.) and Prusa slicer ("PrusaSlicer - Prusa3D - 3D Printers from Josef Prusa," n.d.) are used in the experimental procedure.

Table 1. Results of comparison between the tessellation errors in STL file with different chordal error tolerance

	Minimum deviation	Maximum deviation	Tolerance bound
Surface tessellation with chordal tolerance =0.05 mm	-0.001 mm	0.002 mm	0.003 mm
Surface tessellation with chordal tolerance =0.1 mm	-0.034 mm	0.026 mm	0.060 mm
Surface tessellation with chordal tolerance =0.2 mm	-0.071 mm	0.058 mm	0.129 mm

Fig. 3. Printing results of the aerofoil fabricated based on a STL file generated by 0.05 mm tolerance for the chordal error.

Fig. 4. Printing results of the aerofoil fabricated based on a STL file generated by 0.1 mm tolerance for the chordal error.

3. RESULTS AND DISCUSSIONS

The presented procedure for defining a continuous model and tessellation of the model using triangles are being used for the process of slicing. Constant layer thickness of 0.3 mm is considered to slice the generated STL file. To directly slice the NURBS model, multi-step method is used based on the slope and curvature information from the surface. Fig. 3 – fig. 5 show the aerofoils printed based on the generated STL files with different chordal errors. As can be seen in these pictures, the continuity of the surfaces is highly dependent upon the tessellation procedure. Fig. 6 represents the part fabricated through a direct slicing procedure. The continuity of the surface is considerably improved using the proposed direct slicing approach.

Fig. 5. Printing results of the aerofoil fabricated based on a STL file generated by 0.2 mm tolerance for the chordal error.

Fig. 6. Printing results of the aerofoil fabricated from a direct slicing procedure.

Aerofoil surfaces are scanned using a laser scanner to investigate the accuracies of the fabricated parts. The point clouds extracted from each aerofoil are fitted to the ideal surface. Fig. 7 – Fig. 10 reports the results of fitting process for the scans. For the aerofoil fabricated from the STL file with 0.2 mm chordal error, the minimum deviation is -0.710 mm and maximum deviation is 0.422 mm and in total the part has 1.132 mm deviation as shown in Fig. 7.

The deviations of the part printed based on a STL file with 0.1 mm chordal tolerance, the maximum deviation of 0.349 mm, minimum deviation of -0.666 mm and the total 1.015 mm are found for the part, Fig. 8. As shown in Fig. 9, the final part deviations for the STL file defined with 0.05 mm chordal tolerance are determined as 0.2375 mm for the maximum deviation and -0.686 mm for the minimum deviation. Fig. 10 shows the results of fitting process of the point cloud measured for the surface of the part fabricated through direct slicing procedure. The maximum deviation evaluated from the procedure is determined as 0.392 mm while the minimum deviation is -0.530 mm. The total of the deviations is equal to 0.923 mm.

In addition to improvement to the dimensional accuracy, surface continuity is considerably enhanced which is crucial for the aerodynamic properties of the final parts. The uncertainty of evaluation of the surface continuity based on the discrete results of scanning is high. However, the captured images from the printed parts clearly shows the improvement in the surface continuity of the printed part using the direct slicing approach.

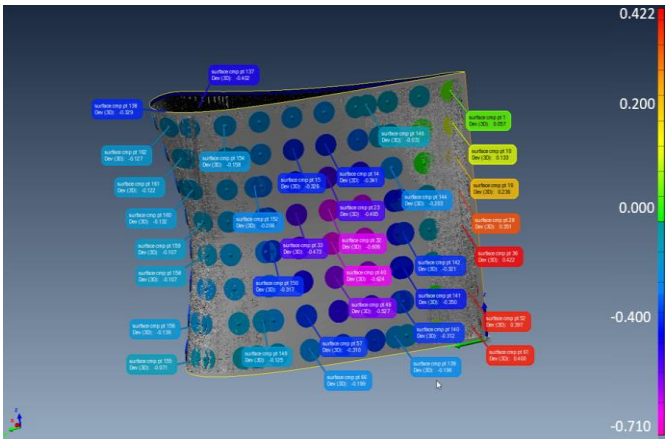

Fig. 7. Fitting results of measured points to the ideal surface when the surface is fabricated from a STL file generated based on 0.2 mm tolerance for the chordal error. Max dev = 0.422 mm, Min dev= -0.710 mm.

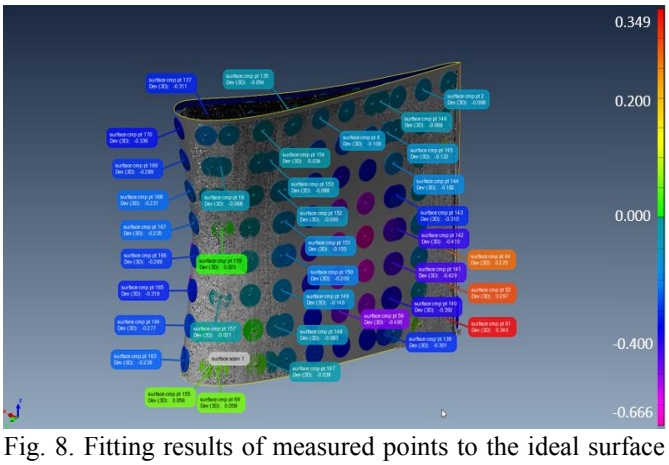

Fig. 8. Fitting results of measured points to the ideal surface when the surface is fabricated from a STL file generated based

on 0.1 mm tolerance for the chordal error. Max dev = 0.349 mm, Min dev= -0.666 mm.

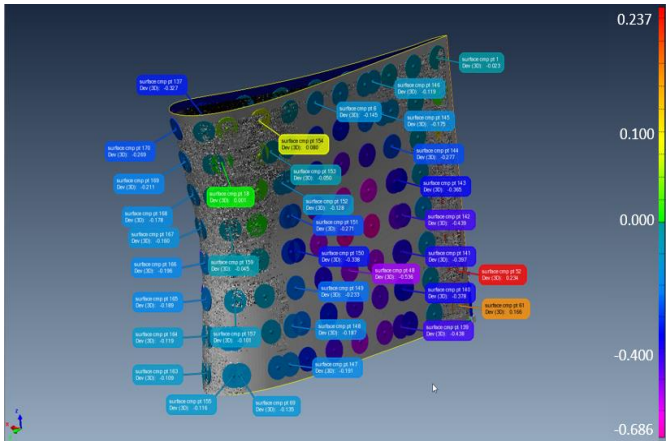

Fig. 9. Fitting results of measured points to the ideal surface when the surface is fabricated from a STL file generated based on 0.05 mm tolerance for the chordal error. Max dev = 0.237 mm, Min dev= -0.686 mm.

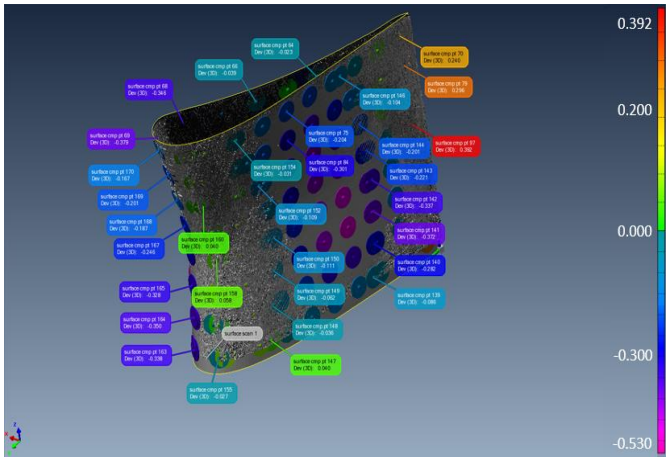

Fig. 10. Fitting results of measured points to the ideal surface when the surface is fabricated directly from a NURBS surface. Max dev = 0.392 mm, Min dev= -0.530 mm.

4. CONCLUSIONS

Process planning is crucial part of an AM process because of its process complexities. An investigation of AM fabricated part accuracies is carried out in this paper. Different source of errors are investigated by comparing the ideal surface with the results of simulations and experimental data. As results show, the accuracy of the model generated by a tessellation procedure is considerably reduced by decreasing the number of triangles. The continuity of the final fabricated part also is highly dependent on the continuity in part surface definition. As the results show, the surface continuity and dimensional accuracy of the part manufactured through a direct slicing procedure is considerably more than the parts produced from STL files. The developed platform for the direct slicing can be used for the process of adaptive slicing using the analytical information of the surface.

REFERENCES

Angelo, L. Di, & Stefano, P. Di. (2010). Computer-Aided Design C 1 continuities detection in triangular meshes. *Computer-Aided Design*, *42*(9), 828–839. https://doi.org/10.1016/j.cad.2010.05.005

Barari, A., Kishawy, H. A., Kaji, F., & Elbestawi, M. A. (2017). On the surface quality of additive manufactured parts. *International Journal of Advanced Manufacturing Technology*, *89*(5–8), 1969–1974. https://doi.org/10.1007/s00170-016-9215-y

Barnhill, R. E., & Kersey, S. N. (1990). A marching method for parametric surface/surface intersection. *Computer Aided Geometric Design*, *7*(1–4), 257–280. https://doi.org/10.1016/0167-8396(90)90035-P

Dolenc, A., & Mäkelä, I. (1994). Slicing procedures for layered manufacturing techniques. *Computer-Aided Design*, *26*(2), 119–126. https://doi.org/10.1016/0010-4485(94)90032-9

Enhanced stl. (2006). *The International Journal of Advanced Manufacturing Technology*, *29*(11–12), 1143–1150.

EP1259711B1 - Aerofoil for an axial flow turbomachine - Google Patents. (n.d.). Retrieved November 12, 2019, from https://patents.google.com/patent/EP1259711B1

Farouki, R. T., Tsai, Y. F., & Yuan, G. F. (1999). Contour machining of free-form surfaces with real-time PH curve CNC interpolators. *Computer Aided Geometric Design*, *16*(1), 61–76. https://doi.org/10.1016/S0167-8396(98)00032-6

Feng, J., Fu, J., Lin, Z., Shang, C., & Li, B. (2018). Direct slicing of T-spline surfaces for additive manufacturing. *Rapid Prototyping Journal*. https://doi.org/10.1108/RPJ-12-2016-0210

Gohari, H, Barari, A., & Kishawy, H. (2016). Using Multistep Methods in Slicing 2 ½ Dimensional Parametric Surfaces for Additive Manufacturing Applications. *IFAC-PapersOnLine*. https://doi.org/10.1016/j.ifacol.2016.12.163

Gohari, Hossein, Barari, A., & Kishawy, H. (2018). An efficient methodology for slicing NURBS surfaces using multi-step methods. *International Journal of Advanced Manufacturing Technology*, *95*(9–12), 3111–3125. https://doi.org/10.1007/s00170-017-1219-8

Gohari, Hossein, Barari, A., Kishawy, H., & Tsuzuki, M. S. G. Intelligent Process Planning for Additive Manufacturing, 52 IFAC-PapersOnLine § (2019). Elsevier B.V. https://doi.org/10.1016/j.ifacol.2019.10.067

Hayasi, M. T., Asiabanpour, B., Hayasi, M. T., & Asiabanpour, · B. (2013). A new adaptive slicing approach for the fully dense freeform fabrication (FDFF) process. *J Intell Manuf*, *24*, 683–694. https://doi.org/10.1007/s10845-011-0615-4

Hiller, J. D., & Lipson, H. (2009). STL 2.0: A Proposal for a Universal Multi-Material Additive Manufacturing File Format. In *Proceedings of Solid Free. Fabrication*

Symposium. SFF'09 Austin (pp. 266–278). Citeseer. Retrieved from http://sffsymposium.engr.utexas.edu/Manuscripts/2009/2009-23-Hiller.pdf%5Cnhttp://sffsymposium.engr.utexas.edu/2009TOC%0Ahttp://utwired.engr.utexas.edu/lff/%0Asymposium/proceedingsArchive/pubs/Manuscripts/2009/2009-23-Hiller.pdf.

Jamiolahmadi, S., & Barari, A. (2014). Surface Topography of Additive Manufacturing Parts Using a Finite Difference Approach. *Journal of Manufacturing Science and Engineering*, *136*(6), 061009. https://doi.org/10.1115/1.4028585

Kumar, C., & Choudhury, A. R. (2005). Volume deviation in direct slicing. *Rapid Prototyping Journal*, *11*(3), 174–184. https://doi.org/10.1108/13552540510601309

Lain, Y. L. (2010). Tool-path generation of planar NURBS curves. *Robotics and Computer-Integrated Manufacturing*, *26*(5), 471–482. https://doi.org/10.1016/j.rcim.2010.03.006

Lalehpour, A., & Barari, A. (2017). Developing skin model in coordinate metrology using a finite element method. *Measurement*, *109*, 149–159. https://doi.org/10.1016/J.MEASUREMENT.2017.05.056

Lalehpour, A., & Barari, A. (2018). A more accurate analytical formulation of surface roughness in layer-based additive manufacturing to enhance the product's precision. *The International Journal of Advanced Manufacturing Technology*, *96*(9–12), 3793–3804. https://doi.org/10.1007/s00170-017-1448-x

Minetto, R., Volpato, N., Stolfi, J., Gregori, R. M. M. H., & da Silva, M. V. G. (2017). An optimal algorithm for 3D triangle mesh slicing. *CAD Computer Aided Design*, *92*, 1–10. https://doi.org/10.1016/j.cad.2017.07.001

Original Prusa i3 MK3S - Prusa3D - 3D Printers from Josef Průša. (n.d.). Retrieved February 11, 2020, from https://www.prusa3d.com/original-prusa-i3-mk3/

Pandey, P. M. P. M. P. M., Reddy, N. V., & Dhande, S. G. S. (2003). Real time adaptive slicing for fused deposition modelling. *International Journal of Machine Tools and Manufacture*, *43*(1), 61–71. https://doi.org/10.1016/S0890-6955(02)00164-5

Paul, R., Design, S. A.-C.-A., & 2015, undefined. (n.d.). A new Steiner patch based file format for additive manufacturing processes. *Elsevier*. Retrieved from https://www.sciencedirect.com/science/article/pii/S0010448515000056

PrusaSlicer - Prusa3D - 3D Printers from Josef Průša. (n.d.). Retrieved February 11, 2020, from https://www.prusa3d.com/prusaslicer/

Sikder, S., Barari, A., & Kishawy, H. A. (2015a). Effect of Adaptive Slicing on Surface Integrity in Additive Manufacturing. In *Volume 1A: 34th Computers and Information in Engineering Conference* (p. V01AT02A052). ASME. https://doi.org/10.1115/detc2014-35559

Sikder, S., Barari, A., & Kishawy, H. A. (2015b). Global adaptive slicing of NURBS based sculptured surface for minimum texture error in rapid prototyping. *Rapid Prototyping Journal*, *21*(6), 649–661. https://doi.org/10.1108/RPJ-09-2013-0090

Starly, B., Lau, A., Sun, W., Lau, W., & Bradbury, T. (2005). Direct slicing of STEP based NURBS models for layered manufacturing. *CAD Computer Aided Design*, *37*(4), 387–397. https://doi.org/10.1016/j.cad.2004.06.014

Tyberg, J., & Bøhn, J. H. (1998). Local adaptive slicing. *Rapid Prototyping Journal*, *4*(3), 118–127. https://doi.org/10.1108/13552549810222993

Umaras, E., & Tsuzuki, M. S. G. (2017). Additive Manufacturing - Considerations on Geometric Accuracy and Factors of Influence. *IFAC-PapersOnLine*, *50*(1), 14940–14945. https://doi.org/10.1016/j.ifacol.2017.08.2545